Review

STZ-Vortex model: The key to understand STZ percolation and shear banding in metallic glasses

D. Şopu [a],[b]

[a] Erich Schmid Institute of Materials Science, Austrian Academy of Sciences, Jahnstraße 12, A-8700 Leoben, Austria
[b] Materials Modelling, Institute of Materials Science, Technical University of Darmstadt, Otto-Berndt-Street 3, 64287 Darmstadt, Germany

ARTICLE INFO

Article history:
Received 30 March 2023
Received in revised form 12 May 2023
Accepted 14 May 2023
Available online 18 May 2023

Keywords:
Metallic glass
Shear band
Shear transformation zone
Molecular dynamics simulations

ABSTRACT

The fast dynamics and localized nature of shear banding together with the disordered structure of metallic glasses make it difficult to gain an understanding of the mechanism of strain localization and shear band formation during deformation. The most widely accepted theory for the atomic-scale mechanisms of shear banding is related to the percolation of shear transformation zones (STZs). Recently we reassessed and clarified the atomistic details of STZs self-assembly mechanisms and provided a new two-unit model crucial in understanding STZs percolation and shear band formation. This manuscript attempts to provide a brief but up-to-date review on the STZ-Vortex mechanism and its applications in the areas of the shear band dynamics and, in general, in the atomistic description of deformation mechanisms in metallic glasses. The review also identifies a number of unsolved issues concerning deformation and relaxation mechanisms in metallic glasses where the STZ-Vortex model could be successfully applied.

Contents

1. Introduction

1.1. Metallic glasses: structure and properties

Unlike crystals, amorphous solids are characterized by the lack of long-range structural order. Amorphous materials are ubiquitous in our daily lives (silica glasses, colloids, gels, granular materials, etc) and span considerable length scales. Metallic glasses have also a disordered structure as in traditional glasses, but their atoms are densely packed via cohesive metallic bonds as in traditional metals [1,2]. This unique combination leads to exceptional properties such as high strength, hardness, and toughness. Hence, metallic glasses are a class of exceptionally strong materials, seen as an ongoing revolution of non-crystalline solid materials and advanced materials in general. Yet, their increased strength comes at the price of reduced ductility, a phenomenon commonly referred to as the inverse strength-ductility paradigm. Below their glass transition and at typical service temperatures, plastic deformation of metallic glasses is highly localized in narrow shear bands. In contrast to crystalline materials, metallic glasses become softer as they are deformed. Shear softening ultimately results in an autocatalytic process of structural disordering and generation of localized excess volume. The strain-softening behavior is the origin of the highly localized, fast character of shear bands that form following yield. The deformation mechanism via shear bands is detrimental, as it promotes premature failure. Thus, understanding and controlling shear band formation and propagation is an essential reference to make metallic glasses useful for a wider range of applications.

The relationship between the structure of metallic glasses and their mechanical behavior is currently lacklustre. The best scientific efforts have been hampered by the difficulty of obtaining precise and well-defined atomic and nanoscale structural information. First, metallic glasses are disordered materials, and unlike crystals, cannot be described by a single structural unit. Second, metallic glasses are thermodynamically out-of-equilibrium materials, making their properties dependent on their thermal history [3,4]. However, learning to find order in disorder allowed to prove the existence of short- and even medium- range order in glassy alloys [5–8–11]. Over time, a variety of environmental descriptors have been proposed to identify and characterize atomic-scale heterogeneities and establish correlations between structural/property fluctuations and the deformation behavior [12–15–18,19]. Nevertheless, there is still much to be done: even the most sophisticated methods, such as those based on machine learning frameworks, cannot satisfactorily characterize the connection between heterogeneities and local plastic events in metallic glasses and establish a universal structure-plasticity picture.

1.2. Tuning the plasticity of metallic glasses

Shear bands are seen as detrimental because they quickly promote fracture, but they can also be advantageous for metallic glasses since they mediate the macroscopic plasticity at room temperature. The difference lies in the ability to control the shear band nucleation and propagation behaviors. Enhanced plasticity can be attained when metallic glasses deform through a organized pattern of multiple shear bands distributed uniformly throughout the structure [20].

To avoid strain localization and formation of critical shear bands, these planar defects must be stabilized, hindered, and/or multiplied. To do this, soft heterogeneities, ranging from nm-size intrinsic structural fluctuations [21–24–27,28] to mm secondary phases [29–32], can be introduced into the structure of the glass. These soft heterogeneities tend to yield earlier, thus acting as initiation sites for a large number of shear bands, which effectively accommodate the applied strain. The generation of a high density of shear bands, which interact with each other and other heterogeneities, can hinder the early failure of the metallic glass composites.

Three strategies have been proposed to control the microstructure and the related mechanical properties in metallic glasses. First, synthesizing composite materials reinforced with a crystalline phase [20,25,29,30,33–36,37,38]. Second, artificial creation of heterogeneous microstructures with controlled morphology by using a variety of mechanical pre-treatments, such as cold rolling [39,40], high-pressure torsion [41] or imprinting [42], chemical treatments to form porous metallic glasses [43–45], or powder compaction [26,46–49,50]. Only recently, a third strategy was proposed that causes irreversible local atomic rearrangements and hence rejuvenation. This can be achieved by many processes, such as elasto-static loading [51–53], cryogenic thermal cycling [54,55] or flash-annealing [56–58]. Rejuvenation of metallic glasses is usually associated with increased disorder, excess free volume (or lower density), increase plasticity and toughness, and reduced hardness and strength [59–62]. However, some rejuvenation processes involving deformation protocols and thermal treatments have revealed increases in density and hardness in some metallic glasses [63–65]. The observed strain-hardening behaviour in these alloys following treatment had been associated with confined microplasticity and local accumulation of irreversible compressive strains [66,67]. Deformation by cold-rolling and shot-peening can promote a transition from softening to hardening behavior which can be correlated to accumulation of compressive residual stresses that overcompensate for free volume generation and associated shear softening [68,69]. Also, simulations of stress modulated metallic glass heterostructures revealed strain hardening together with tensile ductility by only modulating the internal residual stress without altering the structure [70].

1.3. Atomic-scale mechanisms of shear banding

Mixed disorder in metallic glasses is reflected in a complex structural state and elaborate deformation processes. The most widely accepted theory for the atomic-scale mechanisms of shear banding is related to the percolation of shear transformation zones (STZ): groups of atoms that experience larger atomic displacements through cooperative rearrangements under applied stresses [71–73]. These events occur throughout the material, eventually leading to their percolation and formation of a shear band [74–76]. The exact mechanisms and sequence of events which lead to the formation of the shear band are difficult to resolve by experimental means due to their fast dynamics and small dimensions. Argon originally proposed the concept of shear transformations in 1979 [71], but no experiment has so far been able to directly characterize such an elementary event in metallic glasses. Therefore, researchers have relied on computational simulations to observe these events. Molecular dynamics (MD) simulations offer length-scale and temporal resolutions which are most useful to study the task at hand and, in general, are ideal for studying the atomic-level structure-property relationships in metallic glasses.

Two main scenarios for shear band formation have been proposed [2]. The first scenario considers the percolation of homogeneously activated STZ to form localized shear bands [77]. This concept depicts homogeneous nucleation of a shear band from structural fluctuations inherent to the amorphous material itself. The second scenario considers heterogeneous nucleation of shear bands near stress concentrators such as micro- to nano-voids and surface irregularities [78]. Both scenarios suffer the same issue: a lack of establishment of criteria for unambiguous identification of STZ and understanding the mechanism of STZ activation and percolation has not allowed further development of these hypotheses. This is an outstanding problem which has lasted decades. The main goal of this brief review is to answer the key questions regarding STZ activation and percolation processes and improve the understanding of shear bands dynamics in metallic glasses.

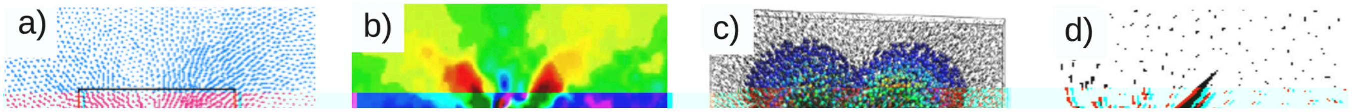

1.4. STZ characteristics

Fundamental and impactful progress towards developing novel tailored metallic glasses with enhanced mechanical properties depends on the ability to control shear banding behaviour. To achieve this ultimate goal one has to reassess and clarify the specific characteristics of STZ and the atomistic details of STZ self-assembly mechanisms. Many particular characteristics of STZ have been provided by simulations in the past decades, such as their geometry and size, their activation energy and also their correlation with the local structure [79–82,83]. Furthermore, atomistic simulations of Lennard-Jones and silicon glasses revealed a quadrupolar distribution of displacement/strain/stress fields around STZ center extending over a much larger space (see Fig. 1) [12,13,82,84–87–90–93,94]. In the athermal limit, all atoms in the system could be considered as a part of the STZ. However, at a finite temperature, because of the thermal noise, above a certain distance from the STZ center it becomes difficult to distinguish between the atomic displacement due to the plastic event and the one due to thermal vibrations. Additionally, due to the complex Eshelby-like morphology and long-range signature of STZs the activation of only a low number of events would results in a long range interaction. The gradient fields overlap to some extent and, may strongly perturb the initial glassy structure and smear out spatial correlations. Hence, the STZ size can thus be only estimated. In the research during the past decades, a fairly wide range of threshold values was chosen to define the STZ size in glasses, resulting to a wide distribution of sizes from a few to a few hundred atoms [79,95–98]. However, if one considering just the center part of the STZ (highlighted in Fig Fig 1a) by the dotted circles), where atoms experience the largest atomic displacements, and exclude the four wings of lower fields that gradually decays when extending into the elastic matrix, then the average size of an STZ is about 2–3 nm and contains several tens of atoms [99,100]. The STZ size is usually comparable the width of a shear band in simulations. Nevertheless, because of spatio-temporal limitations encountered in MD simulations most of these studies focused on the initiation stage of shear banding where the observed structural fluctuation are located at the narrow tip of the shear band. One can surmise that STZ could further growth during shearing approaching larger sizes comparable to the experimental shear band thickness of 10–20 nm.

2. STZ-Vortex mechanism, a novel approach

2.1. Origin of vortex flow units in metallic glasses

Shear bands are not only specific for metallic glasses but they are usually developed within a broad range of materials such as polycrystalline alloys [101], granular materials [102], colloids [103,104], polymers [105], and soils [106]. Within shear bands in these materials, vortex-like structures form in general [107–109]. However, the mechanism for the vortex formation in granular materials can not be applied for metallic glasses.

If one assumes that vortexes could also form in metallic glasses then, one possible origin of the collective rotative motion could be the quadrupolar-like distribution of strain/stress fields around STZ. A schematic representation of the STZ activation is shown in Fig. 2. For simplicity let's assume the activation of one representative STZ: a local squared region in the glass that is plastically deformed. During deformation the squared region is sheared and changes its shape to a rhomboid form. The local distortion results in the generation of a quadruple stress distribution with a compressive component along the longer diagonal (red color) and tensile perpendicular to it (blue color). In analogy to Eshelby's description of an inclusion, such a compression-tensile stress field may be viewed as the long-range effect of the quadrupolar elastic field induced by the STZ in the surrounding material. The directional and coupled stress fields can cause a vortex-like motion of the surrounding atoms between the four wings of the quadrupolar stress field. The rotation field generated by the complex stress distribution around the STZ should also display a quadrupolar distribution while the sign of the rotation is given by the stress field direction: clockwise (red colored arrows) along the shear front and counter clockwise (blue colored arrows) perpendicular to it (see Fig. 2). Next, this hypothesis will be tested and the STZ-Vortex mechanism will be validated by MD simulations.

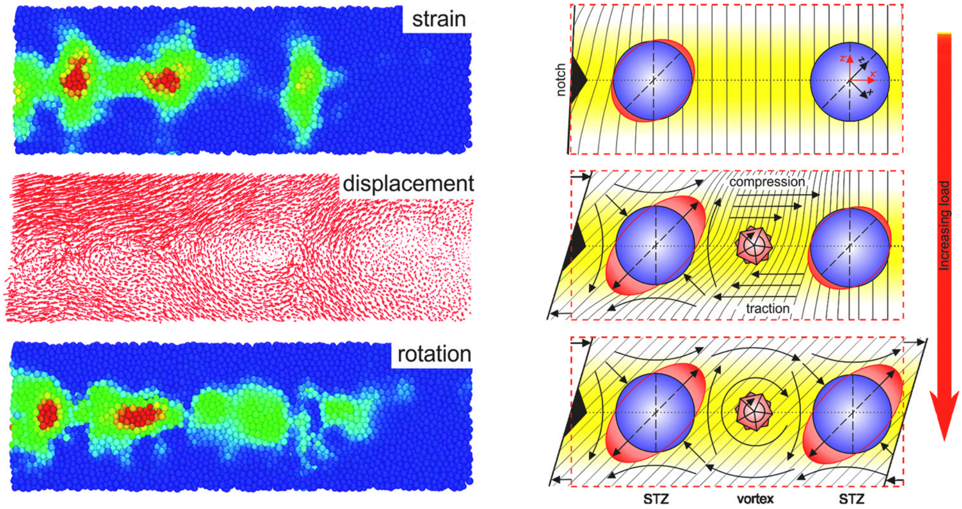

Fig. 3. Left hand side panels display the von Mises strain, displacement vectors and rotation angle (radians) at the tip of the shear band. On the right side a schematic representation of the STZs percolation through the two-unit STZ-Vortex mechanism is shown. The position of the first two STZs are represented by purple circles (not yet activated STZs), whereas STZ distortions (activated STZ) are depicted by orange ellipses. The black arrows indicate atomic motion.
Adapted from Ref. [99] with permission.

2.2. STZs percolation by STZ-Vortex mechanism

It has recently been suggested that the alignment of Eshelby-like quadrupoles may cause the density variation observed in shear bands [110–112]. When closely analyzing a shear band in a MD simulation of $Cu_{64}Zr_{36}$ metallic glass deformed under uniaxial tension (Fig. 3, left hand side panels), we found that the atomic strain distribution within the evolving shear bands is initially highly discontinuous, consisting of isolated regions of larger strain (STZs) [99]. The atomic displacement vectors reveal that atoms between these STZs regions undergo circular displacements in a vortex-like motion (see Fig. 3, middle panel). Moreover, the rotation tensor demonstrates that such vortex-like flow units correspond to a strong rigid rotation of groups of atoms and appears as a signal in the computed micro-rotation field (Fig. 3, lower panel). Thus, we proposed that the mechanism of shear band formation entails two main units: entities characterized by large shear strains (i.e. STZs) and Vortex-like (i.e. rotating) structures. These two units can be identified by analyzing the rotational part of the deformation gradient tensor, which is obtained from a decomposition of the deformation gradient tensor into the rotation matrix and the right stretch tensor [113]. Based on the novel dual STZ-Vortex mechanism it is now possible to discuss the mechanism leading to STZs percolation with much improved detail.

For example, the schematic representation in Fig. 3 (right panels), shows the consecutive activation of neighboring STZs near a notch. For simplicity, the percolation of the first two neighboring STZs is considered (purple circles). At lower loads the first STZ experiences some distortion with negligible effect on the surrounding matrix. At higher loads, the stress at these favorable sites may exceed the threshold value required for STZ activation. The STZ is oriented with the tensile strain along the loading direction, whereas the compressive strain is perpendicular to it, generating a strong antisymmetric stress field in the adjacent material, which in turn causes the observed collective vortex-like motion of the surrounding atoms. Such a vortex-like flow corresponds to a strong rigid rotation of groups of atoms which, in turn, appears to be a necessary step to activate the following STZ through a type of autocatalytic process. The reiteration of the STZ-Vortex unit controls the activation and percolation of STZs and thus the formation of shear bands in metallic glasses.

2.3. STZ-Vortex mechanism at the athermal limit

Removing the thermal noise by simulating athermal quasi-static (AQS) shearing processes allowed to identify and analyze even small strain variations and elastic excitations. At finite temperature, the atomic displacement generated by plastic events could be smaller than the thermal-vibration amplitude that may prevent a refined evaluation of the STZ morphology. Hence, the $Cu_{64}Zr_{36}$ metallic glass sample was deformed by shearing at 0 K [114]. During the shearing process even small variations in the strain/rotations fields could be observed in the early stage of elastic deformation (a representative STZ is highlighted by a dashed square in Fig. 4a, panel (i)). The elastic strain is also non-affine showing heterogeneous characteristics [115,116]. The atomic strain around this elastic event displays a quadrupolar distribution with high values in the middle of the STZ and four wings of lower strain level that gradually decays when extending away from the center (see Fig. 4b). More interestingly, between the four wings of atomic strain the neighboring atoms show a vortex-like motion. The only reasonable explanation for the formation of the vortex flow units is the antisymmetric strain field around STZs. The two perpendicular strain components (compressive vs. tensile) acting at the center of the STZ generate a vortex-like motion of the neighboring atoms located between the four wings of the quadrupolar strain field (see Fig. 4c). The rotation field shows also a quadrupolar distribution. For a better visualization atoms of low strain/rotation have been removed and only half of the STZ is shown (middle panels in Fig. 4b and c). Now it can be seen better that the rotation is very low in the center of the STZ (of high atomic strain) and resembles also a gradient distribution with maxima in the center of each of the four wings.

With further loading, many STZs activate and distribute randomly throughout the entire glassy volume. The initial STZ at stage (i) shows the same rotation magnitude along the deformation process up to the yield point(dashed square at stage (ii) in Fig. 4), which means that the STZ activation is a spontaneously event that could not develop individually further. At the yield point, the stored elastic energy allows for the activation of STZs with higher rotation/strain magnitude. Nevertheless, the STZs activated in the elastic and plastic regimes have similar fingerprints but different magnitudes and dynamics. The activation of STZs in the elastic regime involves small

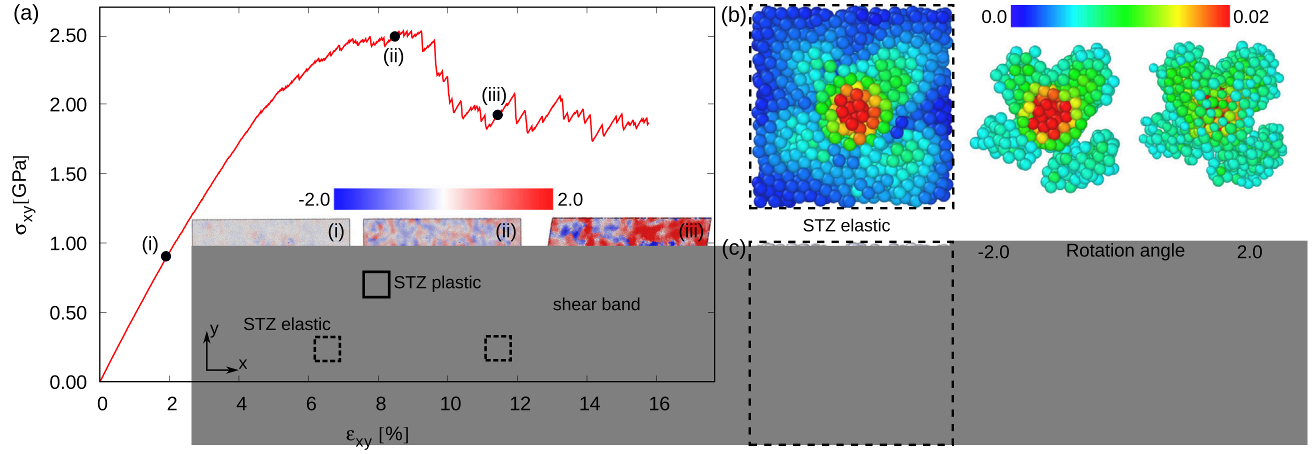

Fig. 4. Stress-strain response, atomic strain and sign of rotation in Cu$_{64}$Zr$_{36}$ metallic glass during athermal quasistatic shearing. (a) Stress-strain curve together with the evolution of the rotation field (in degrees). (i) In the elastic regime the deformation process is highly heterogeneous and mediated by STZs of low strain/rotation fields. (ii) At the yield point, STZs (solid line square) with larger strain/rotation fields activate. (iii) With further shearing a shear band forms. (b) A representative STZ in the elastic regime (highlighted by the dashed square in (a) is shown by the atomic strain and (c), the sign of the rotation angle. The atomic strain around the elastic events show a quadrupolar distribution. The rotation field generated by the complex strain distribution around the STZ shows also a quadrupolar-like shape. For a better visualization atoms of low strain/rotation have been removed and only half of the STZ is shown (middle panels). A 3-dimensional representation of this elastic event is presented in the right-hand side panels.
Reprinted from Ref. [114] with permission.

atomic rearrangements related to bond distortions. Otherwise, STZs at the yield point reveal larger strains and, consequently, much larger rotation fields that increase the probability for STZ percolation and shear band formation [114]. After overcoming the yield point, the autocatalytic iteration of the STZ-Vortex sequence is responsible for the formation of shear bands in metallic glass (Fig. 4a, panel (iii)) [99,100,117].

2.4. STZ-Vortex and anelasticity

According to Argon [118], anelastic behaviour in metallic glasses under loading is related to the local shear transformations. The STZ is embedded in the elastically deformed and more rigid glassy matrix that retains the memory of the initial state. Under unloading process, the elastically deformed matrix exerts back-stresses on the STZ, driving the atomic rearrangement necessary to restore the initial configuration. Nevertheless, in our MD simulations once the external stress is released the glassy structure relaxes just partially and STZs survive the relaxation process (see Fig. 5a). That means, the magnitude of the rotation angle decreases considerably but does not reach zero proving the fact that the recovery of the initial structure is constrained.

An STZ is usually reflected by a stress drop in the stress-strain curve [16]. Such small reductions in stress are already observed in the early stages of the elastic regime (Fig. 5b). After the first observed stress decrease the system is unloaded but the glassy structure relaxes just partially and does not recovery to the initial (zero strain) state. This can be explain by the STZ quadrupolar morphology with long-range signature and the sign of the rotation angle. Given the quadrupolar shape of the strain/rotation fields that gradually extend far from STZ centers, one can consider that these events interact and develop cooperatively. The gradient strain fields overlap to some extent and constrain the atomic rearrangement upon unloading at a later stage and the initial configuration cannot be fully restored. The directional characteristics of the rotation motion, clockwise and counter clockwise (red and blue atoms in Fig. 4c), also affect the relaxation process. When vortexes of opposite rotation directions come into contact their further movement is stopped and the STZ dynamics is perturbed. Consequently, from an early stage of elastic deformation, metallic glasses can not fully recover the initial state when removing the external load. Thus the hypothesis of a purely anelastic deformation in the small deformation regime is disproved.

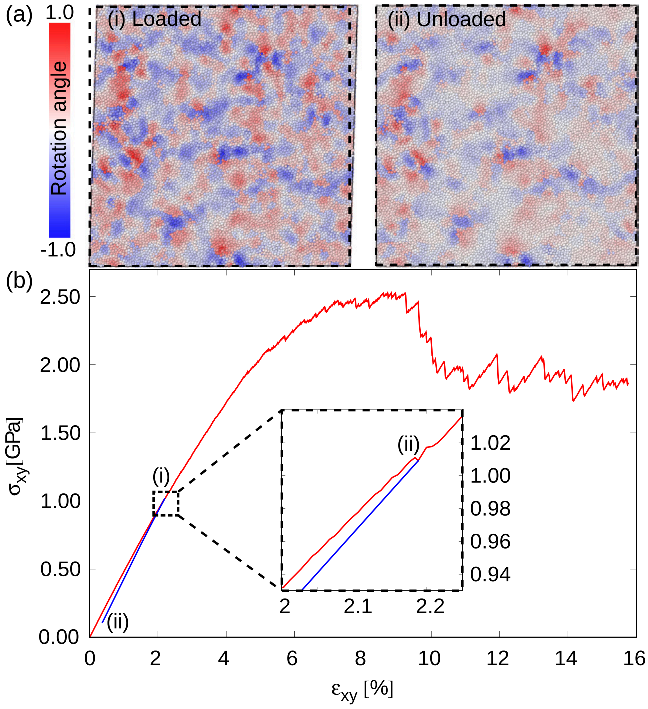

Fig. 5. Residual deformation during the unloading process. (a) Distribution of the angle of rotation (in degree) at a strain level when the first observed decrease in the stress is identified in the stress-strain curve, (b). To better visualize the small variation in the stress during elastic loading (red curve) and unloading process (blue curve) the part of the stress-strain curve corresponding to the dashed box is magnified in the inset panel. The observed residual rotation after relaxation highlights that the structure just partially relaxes.
Adapted from Ref. [114] with permission.

3. Shear banding mechanisms by STZ-Vortex model

Since publication, the novel dual STZ-Vortex mechanism has received considerable recognition and adoption as the mechanism responsible for shear banding [119–122–125,126]. This model has

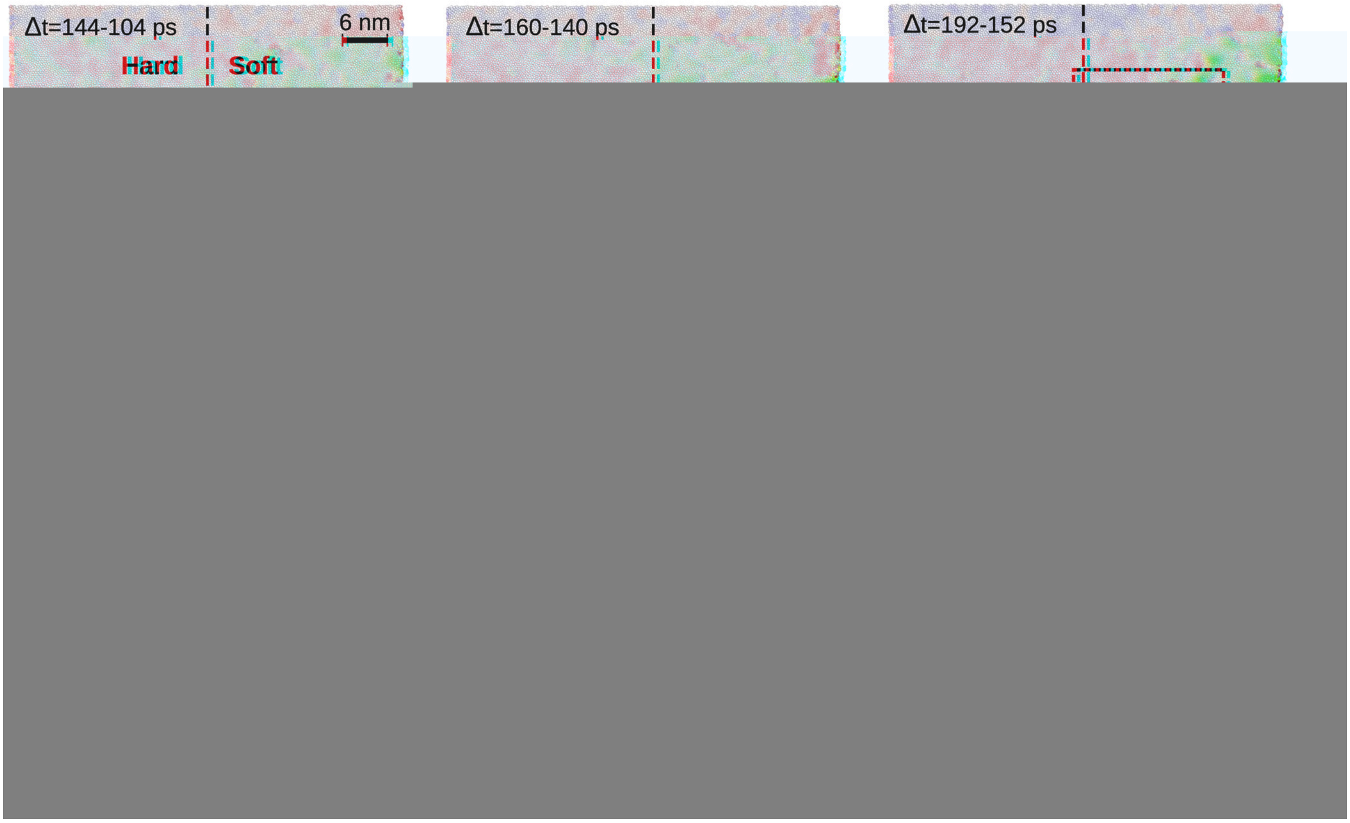

Fig. 6. The sign of rotation angle (in radians) in a two-zone glassy structure upon tensile deformation, where red color corresponds to clockwise rotation and blue color to counter clockwise rotation. To better visualize the variation of STZs axes along the heterostructure the rotation angles corresponding to the dashed boxes are presented in the lower panels.
Adapted from Ref. [100] with permission.

also allowed further development in the areas of the shear band dynamics and atomistic description of deformation mechanisms in metallic glasses, such as shear band formation, interaction [122], their morphology [55,117], branching, multiplication [100], blocking and deflection [58] mechanisms. Furthermore, the STZ-Vortex mechanism has been of paramount importance for understanding the brittle-to-ductile transition, from cracking to localized shear banding [127] and homogeneous deformation [128].

3.1. Shear band branching and multiplication

An effective strategy to attenuate the brittleness of metallic glasses is the introduction of structural heterogeneities. Heterogeneities in terms of harder (denser) and softer glassy (rejuvenated) regions can be generated based on the variety of mechanical and thermal pre-treatments [39,42,129]. The elastic mismatch between structural heterogeneities promote plasticity by inducing shear band branching [119,130]. A major challenge is therefore to understand and control shear band multiplication, a necessary requirement to distribute the strain over a large number of shear bands and thus, provide substantial macroscopic plastic strain. The two-unit STZ-Vortex mechanism has shedded light on the correlation between the strain distribution during deformation and the directional characteristics of the STZ activation process. By simulating a simple dual phase model, consisting of hard and soft glassy regions separated by a planar glass-glass interface, an atomistic description of the shear band branching and multiplication mechanisms have been provided [100]. Fig. 6 illustrates the shear banding mechanism in the dual phase model, where a stress concentrator was created at the surface of the specimen by cutting a small notch. By calculating the sign of the rotation angle with the Y-axis we found that the rotation field shows a quadrupolar distribution: the direction of rotation is clockwise (red color) along the shear front and counter clockwise (blue color) perpendicular to it. Thus, the Eshelby-like rotation field around the STZ can be used as a diagnostic tool to highlight the axes of activated STZs. Above the yield point of the glass a shear band nucleates at the notch tip of the first glassy region and propagates through the two-unit STZ-Vortex mechanism, where STZs display the same inclination angle (left hand side panels in Fig. 6). When a shear band approaches the interface and tries to transit from one region to another, the axes of activated STZs suffer large angle variations restricting the STZs percolation process, resulting in shear band branching and multiplication (middle panels in Fig. 6). The variation of the stress across the interface perturbs the strain distribution and its direction as the shear front advances into the second zone. Basically, STZ-Vortex mechanism characteristic of the hard glass is stopped and STZs with different orientations are activated in the soft region from the tip of the SB in the hard phase (right hand side panels in Fig. 6). The STZ percolation process and shear band propagation in the soft zone follow two new specific directions. In conclusion, a control of the residual stress/strain fields in metallic glasses hinders the shear band propagation and the formation of a critical shear band, that consequently delays shear failure.

3.2. Transition from cracking to shear banding

Some metallic glasses show plasticity under compressive loading, whereas under tensile loading, a sudden catastrophic failure is observed due to highly localized narrow shear band formation [131,132] and cracking perpendicular to the loading direction [133]. Moreover, a systematic atomic-level understanding of the

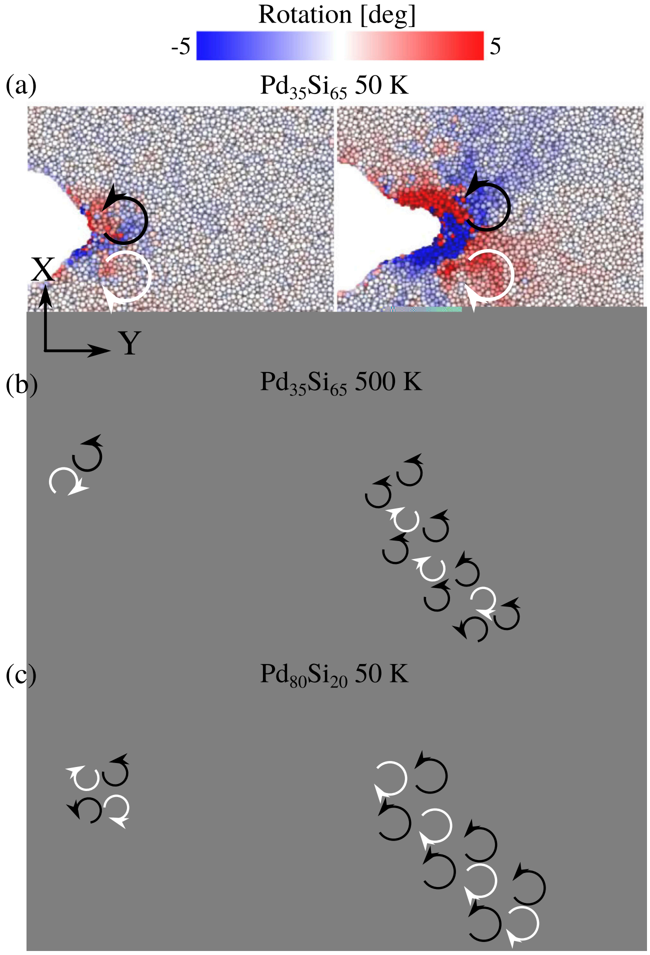

Fig. 7. Atomic scale mechanism of shear band nucleation and cracking resolved by the rotational angle. (a): $Pd_{35}Si_{65}$ at 50 K shows huge rotational displacement at the crack tip, but no STZ activation in the vicinity. (b) and (c): In $Pd_{35}Si_{65}$ at 500 K and $Pd_{80}Si_{20}$ at 50 K the rotational displacements of the atoms lead to STZ activation and shear band formation.
Reprinted from Ref. [127] with permission.

empirically observed embrittlement in metal glasses is lacking. Experimentally, the fracture surface of metallic glasses shows periodic corrugation that suggests crack propagation through nanoscale void formation [126,134]. Void formation and fracture have been correlated to structural fluctuations and the configuration of brittle heterogeneities [135].

In the MD simulations of PdSi metallic glass, a ductile-to-brittle transition from localized shear banding to cracking perpendicular to the loading direction upon tensile loading was observed with increasing silicon content or decreasing the temperature[127]. In this case, the STZ-Vortex model was also applied to explain the transition from shear banding to cracking. At higher temperatures and low Si contents, STZs activate by the displacement of the atoms in the vicinity of the notch tip (Fig. 7b and c). The connected vortex activates the next STZ and the shear band starts to propagate through the sample. However, the atomic displacement at the notch tip does not lead to such STZ activation and shear band formation in Si-rich glass at low temperature (Fig. 7a). Instead, the high stress level at the notch tip triggers breaking of atomic bonds and a crack perpendicular to the loading direction propagates through the sample.

The two initial vortexes that form at the notch develop under loading but the accumulated energy could not overcome the STZ activation energy. Energetic barriers for STZ activation can be overcome by local stresses and thermal vibrations. The above-mentioned transition from cracking to shear banding can be explained by analyzing histograms of activation barriers of STZs for each of these three cases. Activation barriers correlate to the local order and structure in metallic glasses [14]. For $Pb_{80}Si_{20}$ the activation energies are narrowly distributed around 0.01 eV, while $Pb_{35}Si_{65}$ shows a much wider distribution and higher values (Fig. 8). On the other hand, the kinetic energies per atom estimates the probability of thermal activation that increases with temperature. At a low temperature of 50 K, most of the atoms distribute around 0.01 eV kinetic energy per atom, while at 500 K 81% of the atoms have more than 0.01 eV (see Fig. 8) [127]. At low activation barriers the atoms can easily rearrange and the autocatalytic generation of successive STZ and vortex occurs accommodating the external applied strain. Besides, at higher activation barriers the stress level will reach the fracture strength at which bonds are rupturing leaving to crack formation.

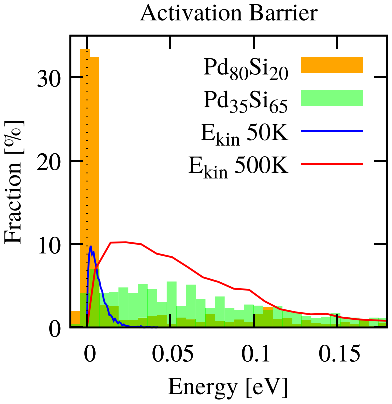

Fig. 8. Histogram of activation energies and average kinetic energy per atom obtained from a saddle point search of the potential energy landscape [136].
Adapted from Ref. [127] with permission.

3.3. Variations in the shear band angle and dynamics

Controlling the shear band dynamics and consequently, improving the plasticity of metallic glasses remain a long-standing challenge. Metallic glasses with improved mechanical properties can be attained by structural engineering such as systematic rejuvenation (in terms of creating free volume) [137] or by controlling the elastic fluctuations and structural heterogeneities [138,139]. The local variations in stress and structure impact on the inclination axes of the STZs, alter their percolation mechanism and consequently affect the shear-band dynamics and kinetics [28]. For instance, by decreasing the temperature from ambient to cryogenic level shear-banding angle increases from 54 to 60° in $Zr_{64.13}Cu_{15.75}Ni_{10.12}Al_{10}$ metallic glass [55,140]. With decreasing temperature, due to the cooling contraction, the overall density increases, while at the atomic scale, the degree of heterogeneity also increases due to the nonaffine thermal contraction [55].

Based on MD simulations and Eshelby inclusion analysis we disclosed the correlation between the structural fluctuations and the change in the stress field around the STZ and the related change in the shear band angle (Fig. 9 upper panels). The repetition of STZ-Vortex arrangements leads to STZ percolation along a preferential direction with an angle of $\alpha 1$ and ultimately results in the formation and propagation of a shear band along this angle (see Fig. 9, upper-left panel). With decreasing the temperature, the nonaffine thermal strain increases and perturbs the stress field around the STZ while the compressive stress becomes larger than the tensile stress (Fig. 9, see upper-right panel). Such a change in the stress distribution will affect the vortex alignment, forcing the shear band to change direction towards a larger angle of $\alpha 2$.

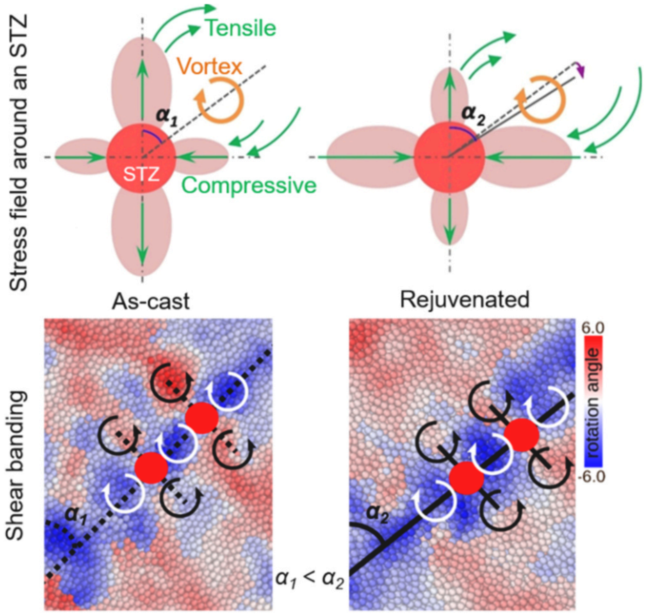

Fig. 9. Upper panels display a schematic representation of the STZ percolation path. Under loading, a quadrupolar-stress field is generated around STZs, showing that the tensile stress (outwards pointing green arrows) acts along the y-direction and a compressive stress (inwards pointing green arrows) occurs perpendicular to it. The dashed lines show the angle of $\alpha1$ (percolation direction of the STZs), and the purple arrows indicate the deviation direction of the angle. Lower panels, MD simulations of SB formation in two different glasses. An increased degree of heterogeneity results in an increase in the shear angle.
Adapted from Ref. [55] with permission.

To verify the importance of soft spots on the deformation behavior and thus validate our model, we performed MD simulations on two kinds of structures, a soft and a hard metallic glass obtained using different cooling rates (Fig. 9 lower panels). The quadrupolar-like distribution of the rotation field around the STZs is used as a diagnostic tool to highlight the axes of the activated STZs. The change in the stress distribution around the STZ directly causes variation in the inclination axes. Hence, the STZ percolation path and shear band formation follow different specific directions, leading to shear band propagation with a higher angle in the soft sample (see lower panels in Fig. 9). Similar correlation between the change in the shear angle and the degree of soft heterogeneities was also observed experimentally [130]. Furthermore, a high degree of heterogeneity slows the rate of STZ percolation and ultimately decelerates shear band sliding enhancing the shear stability [55] In conclusion, the STZ-Vortex model could build a bridge between the discrete features at the atomic-level and the macroscopic properties of metallic glasses.

4. Theory-experiment synergy

Theoretical work, when disconnected from the experiment, often make non-realistic assumptions. Thus, in the past several years, tremendous effort has been made in our group to corroborate results from atomistic simulations with experimental results. Only very recently, by using precession nanodiffraction mapping in the transmission electron microscope, the atomic density and strain distribution of an individual shear band was quantitatively mapped at 2 nm resolution (Fig. 10a) [123]. The shear bands exhibit density alternation from the atomic scale (as also observed in MD simulations) to the submicron scale and complex strain fields exist, causing shear band segmentation and deflection. The map is smoothed and enlarged for better visual quality, as shown in Fig. 10b. Density variation can be observed in the shear band and the glassy matrix. Fig. 10c shows the atomic density variations deduced from the volumetric strain obtained from MD simulation when a shear band has propagated through the specimen. Our combined results highlight a striking resemblance between the structure inside the shear band in simulations and TEM experiments (Fig. 10b and c). Within the shear band, the volumetric strain shows a clear periodicity that correlates to the highly strained regions (STZ clusters) and the vortex-like (rotating) structures repeating at same length scale as the shear band width.

In MD simulations the von Mises strain is used as a diagnostic for identifying STZs [99]. Plotting the value of von Mises strain in a forming shear band as a function of the distance from the shear band tip (Fig. 11a) reveals several peaks of nonaffine deformation. The STZ distortions result in a local dilatation and a net volumetric increase (Fig. 11b). The areas between the activated STZs are, in contrast, characterized by strong rotation and comparatively lower volumetric strains (Fig. 11c). Such a vortex-like structure exhibits a

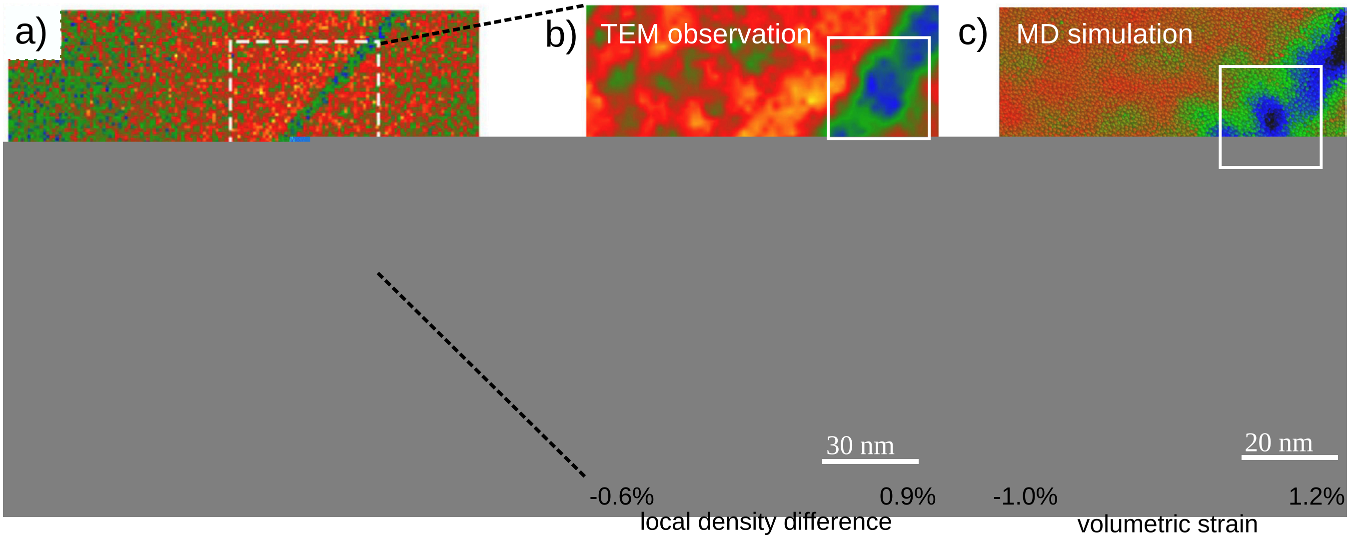

Fig. 10. Fine structures inside the shear band. (a) density difference map from scanning transmission electron microscopy. (b) Magnified views of 2 nm resolution from density difference map from a regions in (a). (c) Atomic density variations obtained from MD simulations highlighting similar fluctuations in density of the shear band. One representative STZ is highlighted for both, experimental and simulated shear band, by the square box.
Adapted from Ref. [123] with permission.

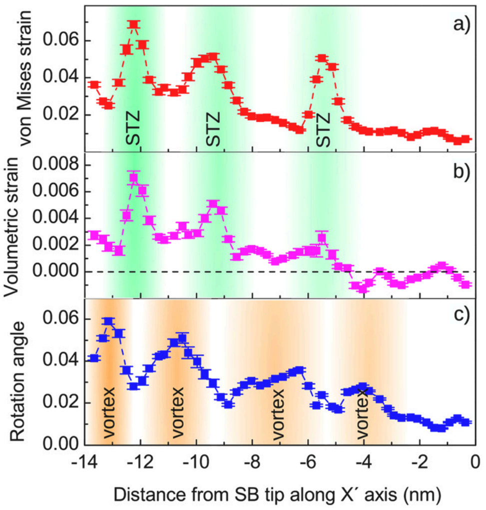

Fig. 11. Values along the shear band direction of (a) von Mises strain, (b) volumetric strain and (c) rotation angle.
Adapted from Ref. [99] with permission.

relatively high fraction of stiff closed-packed full-icosahedral (FI) cluster in its center that explains the local higher densities in these regions[23]. Although for the moment we can not visualize experimentally vortex-like motions, based on the nanoscale structural resembles (theory vs. experiments), one can surmise the validity of STZ-Vortex mechanism and adopt the novel model as a crucial mechanism in understanding STZs percolation and shear band formation. And only very recently, Kang et al. have been shown based on 4-dimensional-STEM that the strain fields percolate in a vortex-like manner building up the shear band [112].

5. Conclusions and future directions

Using molecular dynamics (MD) simulations, we have provided insights into the atomic-level mechanism underlying the shear banding process and proposed a novel two-unit model describing the catalytic self-assembly of STZs. The mechanism is based on the auto-catalytic generation of successive strong strain (STZ) and rotation fields (vortexes). The rotation field generated by the quadrupolar strain distribution around the STZ also shows a quadrupolar distribution between the four wings of the atomic strain. A major advantage of our new model is, that the rotation field around the STZ can be used as a diagnostic tool to highlight the axes of activated STZs while the directional characteristic of the rotation motion defines the shear direction, together having a high impact on the shear band dynamics. The two-unit STZ-Vortex mechanism has the potential to be crucial in understanding STZs percolation and shear band formation. The novel STZ-Vortex model allowed further development in the areas of the shear band dynamics and atomistic description of deformation mechanisms in metallic glasses, such as shear band formation, interaction, their morphology, branching, multiplication, blocking and deflection mechanisms. Also, the STZ-Vortex mechanism provided an atomistic understanding of the brittle-to-ductile transition, from cracking to localized shear banding and homogeneous deformation.

Following the encouraging preliminary results, unresolved issues concerning the two-unit STZ-Vortex mechanism must be further addressed.

1. First, one has to further optimizing and improving the operative STZ-Vortex mechanism. Due to structural fluctuations inherent to the amorphous structure there is a broad distribution of STZ sizes while their fields often overlap. Methods to improve the strain mapping around STZs and highlight the Eshelby-like inclusions characteristics must be established.
2. When comparing the atomic-level mechanisms underlying elastic and plastic deformation there is not a clear transition. Elastic deformation in metallic glasses is a heterogeneous process given the highly heterogeneous nature of the metallic glasses themselves. Insights from elastostatic compression loading support the view of structural rejuvenation at stresses well below the onset of plastic deformation [53]. In the first set of simulations, we have been able to detect reversible events in a very early stage of elastic deformation [114]. Next, several critical questions must be addressed: (i) How can reversible and irreversible events be differentiated? (ii) What is the critical point during elastic deformation where the glassy structure loses memory of the initial state and its initial configuration lost? (iii) What is the magnitude of the strain/rotation fields at which the initially isolated STZs start to dynamically interact and percolate forming shear bands?
3. If one assumes that deformation and structural relaxation are reciprocal processes in tuning the structure of metallic glasses than the STZ-Vortex model could apply to understand and differentiate between different relaxation modes (slow α- and β-relaxation and fast α-relaxation) [141].

Our encouraging first results show great promise to further develop and apply the STZ-Vortex mechanism to metallic glasses, allowing establishment of correlations between structural/elastic fluctuations and local atomic rearrangements during loading in all the range of deformation - from small elastic excitations to fracture. These theoretical developments and the synergistic combination of atomistic modeling and advanced experiments could build a bridge between the discrete features at the atomic-level and the macroscopic properties of metallic glasses and overcome the inverse strength-ductility paradigm.

Data Availability

Data will be made available on request.

Declaration of Competing Interest

The authors declare that they have no known competing financial interests or personal relationships that could have appeared to influence the work reported in this paper.

Acknowledgment

This brief review is part of the special issue dedicated to Prof. Jürgen Eckert honouring him on his 60th birthday. At this point, I would like to thank Prof. Jürgen Eckert for all the support and guidance offered in recent years. The author acknowledges financial support by the Deutsche Forschungsgemeinschaft (DFG) through Grant no. SO 1518/1-1 and European Research Council under the ERC Advanced Grant INTELHYB (grant ERC-2013-ADG-340025). The author is thankful to his research students, Franco Moitzi and Dr. Xudong Yuan and collaborators, Dr. Sergio Scudino, Dr. Mihai Stoica, Dr. Alexander Stukowski, Dr. Xilei Bian, Dr. Florian Speickermann and Dr. Christoph Gammer for helpful discussions and their contributions to the work reviewed in this article. The author is grateful for the computing time granted during the years by the Lichtenberg high performance computer of Technische Universität Darmstadt and by the John von Neumann Institute for Computing (NIC) and provided on the supercomputer JURECA at the Juelich Supercomputing Centre (JSC).

References

[1] A.L. Greer, Metallic glasses, Science 267 (5206) (1995) 1947–1953.

[2] A.L. Greer, Y.Q. Cheng, E. Ma, Shear bands in metallic glasses, Mater. Sci. Eng. R. Rep. 74 (4) (2013) 71–132 ⟨http://www.sciencedirect.com/science/article/pii/S0927796×13000259⟩.

[3] A.L. Cahn, R.W. Greer, Metastable states of alloys, Phys. Metall. Elsevier Sci. (1996) 1724.

[4] S.V. Khonik, A.V. Granato, D.M. Joncich, A. Pompe, V.A. Khonik, Evidence of distributed interstitialcy-like relaxation of the shear modulus due to structural relaxation of metallic glasses, Phys. Rev. Lett. 100 (6) (2008) 065501.

[5] H. Jonsson, H.C. Andersen, Icosahedral ordering in the lennard-jones liquid and glass, Phys. Rev. Lett. 60 (22) (1988) 2295–2298, https://doi.org/10.1103/PhysRevLett.60.2295

[6] D.B. Miracle, A structural model for metallic glasses, Nat. Mater. 3 (10) (2004) 697–702.

[7] Z.W. Wu, F.X. Li, C.W. Huo, M.Z. Li, W.H. Wang, K.X. Liu, Critical scaling of icosahedral medium-range order in cuzr metallic glass-forming liquids, Sci. Rep. 6 (1) (2016) 35967, https://doi.org/10.1038/srep35967

[8] Y.Q. Cheng, A.J. Cao, H.W. Sheng, E. Ma, Local order influences initiation of plastic flow in metallic glass: effects of alloy composition and sample cooling history, Acta Mater. 56 (18) (2008) 5263–5275.

[9] Y. Ritter, K. Albe, Chemical and topological order in shear bands of cu64zr36 and cu36zr64 glasses, J. Appl. Phys. 111 (10) (2012) 103527, https://doi.org/10.1063/1.4717748

[10] A. Hirata, P.F. Guan, T. Fujita, Y. Hirotsu, A. Inoue, A.R. Yavari, T. Sakurai, M.W. Chen, Direct observation of local atomic order in a metallic glass, Nat. Mater. 10 (2011) 28–33.

[11] A. Hirata, L.J. Kang, T. Fujita, B. Klumov, K. Matsue, M. Kotani, A.R. Yavari, M.W. Chen, Geometric frustration of icosahedron in metallic glasses, Science 341 (6144) (2013) 376–379, https://doi.org/10.1126/science.1232450 ⟨http://science.sciencemag.org/content/341/6144/376.full.pdf⟩ http://science.sciencemag.org/content/341/6144/376.

[12] M. Tsamados, A. Tanguy, F. Léonforte, J.L. Barrat, On the study of local-stress rearrangements during quasi-static plastic shear of a model glass: do local-stress components contain enough information? Eur. Phys. J. E 26 (3) (2008) 283–293, https://doi.org/10.1140/epje/i2007-10324-y

[13] D. Rodney, A. Tanguy, D. Vandembroucq, Modeling the mechanics of amorphous solids at different length scale and time scale, Model. Simul. Mater. Sci. Eng. 19 (8) (2011) 083001, https://doi.org/10.1088/0965-0393/19/8/083001

[14] J. Ding, Y.-Q. Cheng, H. Sheng, M. Asta, R.O. Ritchie, E. Ma, Universal structural parameter to quantitatively predict metallic glass properties, Nat. Commun. 7 (2016) 13733, https://doi.org/10.1038/ncomms13733

[15] C.-X. Peng, D. Şopu, K.-K. Song, Z.-T. Zhang, L. Wang, J. Eckert, Bond length deviation in cuzr metallic glasses, Phys. Rev. B 96 (17) (2017) 174112, https://doi.org/10.1103/PhysRevB.96.174112

[16] A. Barbot, M. Lerbinger, A. Hernandez-Garcia, R. Garcia-Garcia, M.L. Falk, D. Vandembroucq, S. Patinet, Local yield stress statistics in model amorphous solids, Phys. Rev. E 97 (3) (2018) 033001, https://doi.org/10.1103/PhysRevE.97.033001

[17] D. Richard, M. Ozawa, S. Patinet, E. Stanifer, B. Shang, S.A. Ridout, B. Xu, G. Zhang, P.K. Morse, J.-L. Barrat, L. Berthier, M.L. Falk, P. Guan, A.J. Liu, K. Martens, S. Sastry, D. Vandembroucq, E. Lerner, M.L. Manning, Predicting plasticity in disordered solids from structural indicators, Phys. Rev. Mater. 4 (11) (2020) 113609, https://doi.org/10.1103/PhysRevMaterials.4.113609

[18] P.M. Piaggi, M. Parrinello, Entropy based fingerprint for local crystalline order, J. Chem. Phys. 147 (11) (2017) 114112, https://doi.org/10.1063/1.4998408

[19] J.C. Qiao, Q. Wang, J.M. Pelletier, H. Kato, R. Casalini, D. Crespo, E. Pineda, Y. Yao, Y. Yang, Structural heterogeneities and mechanical behavior of amorphous alloys, Prog. Mater. Sci. 104 (2019) 250–329 ⟨http://www.sciencedirect.com/science/article/pii/S0079642519300428⟩.

[20] K. Albe, Y. Ritter, D. Şopu, Enhancing the plasticity of metallic glasses: shear band formation, nanocomposites and nanoglasses investigated by molecular dynamics simulations, Mech. Mater. 67 (0) (2013) 94–103, https://doi.org/10.1016/j.mechmat.2013.06.004 ⟨http://www.sciencedirect.com/science/article/pii/S0167663613001117⟩.

[21] D. Magagnosc, G. Kumar, J. Schroers, P. Felfer, J. Cairney, D. Gianola, Effect of ion irradiation on tensile ductility, strength and fictive temperature in metallic glass nanowires, Acta Mater. 74 (2014) 165–182, https://doi.org/10.1016/j.actamat.2014.04.002 ⟨http://www.sciencedirect.com/science/article/pii/S1359645414002419⟩.

[22] T. Brink, M. Peterlechner, H. Rösner, K. Albe, G. Wilde, Influence of crystalline nanoprecipitates on shear-band propagation in cu-zr-based metallic glasses, Phys. Rev. Appl. 5 (2016) 054005, https://doi.org/10.1103/PhysRevApplied.5.054005

[23] Y.Q. Cheng, E. Ma, H.W. Sheng, Atomic level structure in multicomponent bulk metallic glass, Phys. Rev. Lett. 102 (24) (2009) 245501.

[24] J. Eckert, A. Reger-Leonhard, B. Weiss, M. Heilmaier, Nanostructured materials in multicomponent alloy systems, Mater. Sci. Eng., A 301 (1) (2001) 1–11.

[25] C. Fan, A. Inoue, Improvement of mechanical properties by precipitation of nanoscale compound particles in zr-cu-pd-al amorphous alloys, Mater. Trans., JIM 38 (12) (1997) 1040–1046.

[26] J.X. Fang, U. Vainio, W. Puff, R. Würschum, X.L. Wang, D. Wang, M. Ghafari, F. Jiang, J. Sun, H. Hahn, H. Gleiter, Atomic structure and structural stability of sc75fe25 nanoglasses, Nano Lett. 12 (1) (2012) 458–463, https://doi.org/10.1021/nl2038216

[27] H. Gleiter, T. Schimmel, H. Hahn, Nanostructured solids - from nano-glasses to quantum transistors, Nano Today 9 (1) (2014) 17–68 ⟨http://www.sciencedirect.com/science/article/pii/S1748013214000243⟩.

[28] Y. Wang, C. Lee, J. Yi, X. An, M. Pan, K. Xie, X. Liao, J. Cairney, S. Ringer, W. Wang, Ultrahigh-strength submicron-sized metallic glass wires, Scr. Mater. 84–85 (2014) 27–30, https://doi.org/10.1016/j.scriptamat.2014.04.005 ⟨http://www.sciencedirect.com/science/article/pii/S135964621400150X⟩.

[29] C.C. Hays, C.P. Kim, W.L. Johnson, Microstructure controlled shear band pattern formation and enhanced plasticity of bulk metallic glasses containing in situ formed ductile phase dendrite dispersions, Phys. Rev. Lett. 84 (13) (2000) 2901–2904.

[30] J. Eckert, J. Das, S. Pauly, C. Duhamel, Mechanical properties of bulk metallic glasses and composites, J. Mater. Res. 22 (2007) 285–301, https://doi.org/10.1557/jmr.2007.0050 ⟨http://journals.cambridge.org/article_S0884291400092554⟩.

[31] Z. Liu, R. Li, G. Liu, K. Song, S. Pauly, T. Zhang, J. Eckert, Pronounced ductility in cuzral ternary bulk metallic glass composites with optimized microstructure through melt adjustment, AIP Adv. 2 (3) (2012), https://doi.org/10.1063/1.4754853

[32] S. Cardinal, J.M. Pelletier, G.Q. Xie, F. Mercier, F. Dalmas, Enhanced compressive plasticity in a cu-zr-al - based metallic glass composite, J. Alloy. Compd. 782 (2019) 59–68 ⟨https://www.sciencedirect.com/science/article/pii/S0925838818344323⟩.

[33] C.C. Hays, C.P. Kim, W.L. Johnson, Improved mechanical behavior of bulk metallic glasses containing in situ formed ductile phase dendrite dispersions, Mater. Sci. Eng., A 304 (2001) 650–655.

[34] G. He, J. Eckert, W. Löser, L. Schultz, Novel ti-base nanostructure-dendrite composite with enhanced plasticity, Nat. Mater. 2 (1) (2003) 33–37.

[35] S. Pauly, S. Gorantla, G. Wang, U. Kühn, J. Eckert, Transformation-mediated ductility in cuzr-based bulk metallic glasses, Nat. Mater. 9 (6) (2010) 473–477.

[36] S. Pauly, G. Liu, S. Gorantla, G. Wang, U. Kühn, D.H. Kim, J. Eckert, Criteria for tensile plasticity in cu-zr-al bulk metallic glasses, Acta Mater. 58 (14) (2010) 4883–4890.

[37] D. Şopu, M. Stoica, J. Eckert, Deformation behavior of metallic glass composites reinforced with shape memory nanowires studied via molecular dynamics simulations, Appl. Phys. Lett. 106 (21) (2015), https://doi.org/10.1063/1.4921857

[38] D. Şopu, X. Yuan, F. Moitzi, M. Stoica, J. Eckert, Structure-property relationships in shape memory metallic glass composites, Materials 12 (9) (2019).

[39] M.H. Lee, K.S. Lee, J. Das, J. Thomas, U. Kühn, J. Eckert, Improved plasticity of bulk metallic glasses upon cold rolling, Scr. Mater. 62 (9) (2010) 678–681.

[40] Q.P. Cao, J.W. Liu, K.J. Yang, F. Xu, Z.Q. Yao, A. Minkow, H.J. Fecht, J. Ivanisenko, L.Y. Chen, X.D. Wang, S.X. Qu, J.Z. Jiang, Effect of pre-existing shear bands on the tensile mechanical properties of a bulk metallic glass, Acta Mater. 58 (4) (2010) 1276–1292.

[41] S.-H. Joo, D.-H. Pi, A.D.H. Setyawan, H. Kato, M. Janecek, Y.C. Kim, S. Lee, H.S. Kim, Work-hardening induced tensile ductility of bulk metallic glasses via high-pressure torsion, Sci. Rep. 5 (2015) 9660 ⟨http://www.ncbi.nlm.nih.gov/pmc/articles/PMC5386117/⟩.

[42] S. Scudino, B. Jerliu, S. Pauly, K. Surreddi, U. Kühn, J. Eckert, Ductile bulk metallic glasses produced through designed heterogeneities, Scr. Mater. 65 (9) (2011) 815–818, https://doi.org/10.1016/j.scriptamat.2011.07.039 ⟨http://www.sciencedirect.com/science/article/pii/S1359646211004386⟩.

[43] A. Brothers, D. Dunand, Amorphous metal foams, Scr. Mater. 54 (4) (2006) 513–520, https://doi.org/10.1016/j.scriptamat.2005.10.048 ⟨http://www.sciencedirect.com/science/article/pii/S1359646205006871⟩.

[44] A. Inoue, T. Wada, D.V. Louzguine-Luzgin, Improved mechanical properties of bulk glassy alloys containing spherical pores, Mater. Sci. Eng.: A 471 (1–2) (2007) 144–150, https://doi.org/10.1016/j.msea.2006.10.172 ⟨http://www.sciencedirect.com/science/article/pii/S0921509307004571⟩.

[45] M. Myers, S. Charnvanichborikarn, C. Wei, Z. Luo, G. Xie, S. Kucheyev, D. Lucca, L. Shao, Phase transition, segregation and nanopore formation in high-energy heavy-ion-irradiated metallic glass, Scr. Mater. 67 (11) (2012) 887–890, https://doi.org/10.1016/j.scriptamat.2012.08.015 ⟨http://www.sciencedirect.com/science/article/pii/S1359646212005258⟩.

[46] J. Jing, A. Kramer, R. Birringer, H. Gleiter, U. Gonser, Modified atomic structure in a pd-fe-si nanoglass: a mössbauer study, J. Non-Cryst. Solids 113 (2–3) (1989) 167–170 ⟨http://www.sciencedirect.com/science/article/B6TXM-48CXMM7-V3/2/0f05e9baad09654aa30abff391ba440a⟩.

[47] D. Şopu, K. Albe, Y. Ritter, H. Gleiter, From nanoglasses to bulk massive glasses, Appl. Phys. Lett. 94 (19) (2009) 191911, https://doi.org/10.1063/1.3130209

[48] D. Şopu, Y. Ritter, H. Gleiter, K. Albe, Deformation behavior of bulk and nanostructured metallic glasses studied via molecular dynamics simulations, Phys. Rev. B 83 (2011) 100202, https://doi.org/10.1103/PhysRevB.83.100202

[49] O. Adjaoud, K. Albe, Influence of microstructural features on the plastic deformation behavior of metallic nanoglasses, Acta Mater. 168 (2019) 393–400 ⟨https://www.sciencedirect.com/science/article/pii/S1359645419301193⟩.

[50] O. Franke, D. Leisen, H. Gleiter, H. Hahn, Thermal and plastic behavior of nanoglasses, J. Mater. Res. 29 (10) (2014) 1210–1216, https://doi.org/10.1557/jmr.2014.101

[51] S.-J. Lee, B.-G. Yoo, J.-I. Jang, J.-C. Lee, Irreversible structural change induced by elastostatic stress imposed on an amorphous alloy and its influence on the mechanical properties, Met. Mater. Int. 14 (1) (2008) 9, https://doi.org/10.3365/met.mat.2008.02.009

[52] K.W. Park, Effect of the atomic packing density on the structural change rate of amorphous alloys under elastostatic stress, Met. Mater. Int. 14 (2) (2008) 159–163, https://doi.org/10.3365/met.mat.2008.04.159

[53] K.-W. Park, C.-M. Lee, M. Wakeda, Y. Shibutani, M.L. Falk, J.-C. Lee, Elastostatically induced structural disordering in amorphous alloys, Acta Mater. 56 (19) (2008) 5440–5450 ⟨http://www.sciencedirect.com/science/article/pii/S1359645408005168⟩.

[54] S.V. Ketov, Y.H. Sun, S. Nachum, Z. Lu, A. Checchi, A.R. Beraldin, H.Y. Bai, W.H. Wang, D.V. Louzguine-Luzgin, M.A. Carpenter, A.L. Greer, Rejuvenation of metallic glasses by non-affine thermal strain, Nature 524 (7564) (2015) 200–203, https://doi.org/10.1038/nature14674

[55] X. Bian, D. Şopu, G. Wang, B. Sun, J. Bednarcik, C. Gammer, Q. Zhai, J. Eckert, Signature of local stress states in the deformation behavior of metallic glasses, NPG Asia Mater. 12 (1) (2020) 59, https://doi.org/10.1038/s41427-020-00241-4

[56] K. Kosiba, S. Pauly, Inductive flash-annealing of bulk metallic glasses, Sci. Rep. 7 (1) (2017) 2151, https://doi.org/10.1038/s41598-017-02376-x

[57] S. Küchemann, P.M. Derlet, C. Liu, D. Rosenthal, G. Sparks, W.S. Larson, R. Maaß, Energy storage in metallic glasses via flash annealing, Adv. Funct. Mater. 28 (50) (2018) 1805385.

[58] K. Kosiba, D. Şopu, S. Scudino, L. Zhang, J. Bednarcik, S. Pauly, Modulating heterogeneity and plasticity in bulk metallic glasses: Role of interfaces on shear banding, Int. J. Plast. 119 (2019) 156–170 ⟨http://www.sciencedirect.com/science/article/pii/S0749641918304170⟩.

[59] W. Dmowski, Y. Yokoyama, A. Chuang, Y. Ren, M. Umemoto, K. Tsuchiya, A. Inoue, T. Egami, Structural rejuvenation in a bulk metallic glass induced by severe plastic deformation, Acta Mater. 58 (2) (2010) 429–438, https://doi.org/10.1016/j.actamat.2009.09.021 ⟨http://www.sciencedirect.com/science/article/pii/S135964540900617X⟩.

[60] J.W. Liu, Q.P. Cao, L.Y. Chen, X.D. Wang, J.Z. Jiang, Shear band evolution and hardness change in cold-rolled bulk metallic glasses, Acta Mater. 58 (14) (2010) 4827–4840 ⟨https://www.sciencedirect.com/science/article/pii/S1359645410002934⟩.

[61] X. Yuan, D. Şopu, K. Song, J. Eckert, Relaxation and strain-hardening relationships in highly rejuvenated metallic glasses (2022).

[62] X. Yuan, D. Şopu, F. Spieckermann, K.K. Song, S.V. Ketov, K.G. Prashanth, J. Eckert, Maximizing the degree of rejuvenation in metallic glasses, Scr. Mater. 212 (2022) 114575⟨https://www.sciencedirect.com/science/article/pii/S1359646222000756⟩.

[63] T. Ge, C. Wang, J. Tan, T. Ma, X. Yu, C. Jin, W. Wang, H. Bai, Unusual energy state evolution in ce-based metallic glass under high pressure, J. Appl. Phys. 121 (20) (2017) 205109, https://doi.org/10.1063/1.4983017

[64] C. Wang, Z. Yang, T. Ma, Y. Sun, Y. Yin, Y. Gong, L. Gu, P. Wen, P. Zhu, Y. Long, High stored energy of metallic glasses induced by high pressure, Appl. Phys. Lett. 110 (11) (2017) 111901, https://doi.org/10.1063/1.4978600

[65] N. Miyazaki, M. Wakeda, Y.J. Wang, S. Ogata, Prediction of pressure-promoted thermal rejuvenation in metallic glasses, Npj Comput. Mater. 2 (1) (2016) 1–9, https://doi.org/10.1038/npjcompumats.2016.13

[66] C. Deng, C.A. Schuh, Atomistic mechanisms of cyclic hardening in metallic glass, Appl. Phys. Lett. 100 (25) (2012) 251909, https://doi.org/10.1063/1.4729941

[67] D. Zhao, H. Zhao, B. Zhu, S. Wang, Investigation on hardening behavior of metallic glass under cyclic indentation loading via molecular dynamics simulation, Appl. Surf. Sci. 416 (2017) 14–23 ⟨https://www.sciencedirect.com/science/article/pii/S0169433217311522⟩.

[68] M. Stolpe, J.J. Kruzic, R. Busch, Evolution of shear bands, free volume and hardness during cold rolling of a zr-based bulk metallic glass, Acta Mater. 64 (2014) 231–240 ⟨https://www.sciencedirect.com/science/article/pii/S1359645413007982⟩.

[69] Y. Zhang, W.H. Wang, A.L. Greer, Making metallic glasses plastic by control of residual stress, Nat. Mater. 5 (11) (2006) 857–860, https://doi.org/10.1038/nmat1758

[70] X. Yuan, D. Şopu, J. Eckert, Origin of strain hardening in monolithic metallic glasses, Phys. Rev. B 103 (14) (2021) L140107, https://doi.org/10.1103/PhysRevB.103.L140107

[71] A.S. Argon, Plastic-deformation in metallic glasses, Acta Metall. 27 (1) (1979) 47–58.

[72] C.A. Schuh, A.C. Lund, Atomistic basis for the plastic yield criterion of metallicglass, Nat. Mater. 2 (7) (2003) 449–452, https://doi.org/10.1038/nmat918

[73] F. Spaepen, Microscopic mechanism for steady-state inhomogeneous flow in metallic glasses, Acta Metall. 25 (4) (1977) 407–415.

[74] Y.F. Shi, M.L. Falk, Strain localization and percolation of stable structure in amorphous solids rid b-3278-2008 rid a-8478-2008, Phys. Rev. Lett. 95 (9) (2005) 095502.

[75] Y.F. Shi, M.L. Falk, Atomic-scale simulations of strain localization in three-dimensional model amorphous solids, Phys. Rev. B 73 (21) (2006) 214201.

[76] Y.S. Wang, G.J. Hao, Y. Zhang, J.P. Lin, L. Song, J.W. Qiao, The role of the interface in a ti-based metallic glass matrix composite with in situ dendrite reinforcement, Surf. Interface Anal. 46 (5) (2014) 293–296, https://doi.org/10.1002/sia.5413

[77] F. Shimizu, S. Ogata, J. Li, Theory of shear banding in metallic glasses and molecular dynamics calculations, Mater. Trans. 48 (11) (2007) 2923–2927.

[78] F. Shimizu, S. Ogata, J. Li, Yield point of metallic glass, Acta Mater. 54 (16) (2006) 4293–4298, https://doi.org/10.1016/j.actamat.2006.05.024 ⟨http://www.sciencedirect.com/science/article/pii/S1359645406003600⟩.

[79] M. Zink, K. Samwer, W.L. Johnson, S.G. Mayr, Validity of temperature and time equivalence in metallic glasses during shear deformation, Phys. Rev. B 74 (1) (2006) 012201.

[80] S.G. Mayr, Activation energy of shear transformation zones: a key for understanding rheology of glasses and liquids, Phys. Rev. Lett. 97 (19) (2006) 195501, https://doi.org/10.1103/PhysRevLett.97.195501 ⟨http://link.aps.org/abstract/PRL/v97/e195501⟩.

[81] F. Delogu, Strain localization in metallic amorphous/amorphous composites, Intermetallics 16 (7) (2008) 904–909.

[82] D. Rodney, C. Schuh, Distribution of thermally activated plastic events in a flowing glass, Phys. Rev. Lett. 102 (23) (2009) 235503, https://doi.org/10.1103/PhysRevLett.102.235503

[83] P.G. Debenedetti, F.H. Stillinger, Supercooled liquids and the glass transition, Nature 410 (6825) (2001) 259–267, https://doi.org/10.1038/35065704

[84] V.V. Bulatov, A.S. Argon, A stochastic model for continuum elasto-plastic behavior. i. numerical approach and strain localization, Model. Simul. Mater. Sci. Eng. 2 (2) (1994) 167 ⟨http://stacks.iop.org/0965-0393/2/i=2/a=001⟩.

[85] C.E. Maloney, A. Lemaitre, Amorphous systems in athermal, quasistatic shear, Phys. Rev. E 74 (1) (2006) 016118, https://doi.org/10.1103/PhysRevE.74.016118

[86] R. Dasgupta, H.G.E. Hentschel, I. Procaccia, Microscopic mechanism of shear bands in amorphous solids, Phys. Rev. Lett. 109 (2012) 255502, https://doi.org/10.1103/PhysRevLett.109.255502

[87] R. Dasgupta, H.G.E. Hentschel, I. Procaccia, Yield strain in shear banding amorphous solids, Phys. Rev. E 87 (2013) 022810, https://doi.org/10.1103/PhysRevE.87.022810

[88] A. Tanguy, F. Leonforte, J.L. Barrat, Plastic response of a 2d lennard-jones amorphous solid: detailed analysis of the local rearrangements at very slow strain rate, Eur. Phys. J. E 20 (3) (2006) 355–364, https://doi.org/10.1140/epje/i2006-10024-2

[89] C. Goldenberg, A. Tanguy, J.-L. Barrat, Particle displacements in the elastic deformation of amorphous materials: local fluctuations vs. non-affine field, Europhys. Lett. 80 (1) (2007) 16003, https://doi.org/10.1209/0295-5075/80/16003

[90] C. Fusco, T. Albaret, A. Tanguy, Role of local order in the small-scale plasticity of model amorphous materials, Phys. Rev. E 82 (6) (2010) 066116, https://doi.org/10.1103/PhysRevE.82.066116

[91] T. Albaret, A. Tanguy, F. Boioli, D. Rodney, Mapping between atomistic simulations and eshelby inclusions in the shear deformation of an amorphous silicon model, Phys. Rev. E 93 (5) (2016) 053002, https://doi.org/10.1103/PhysRevE.93.053002

[92] P. Schall, D.A. Weitz, F. Spaepen, Structural rearrangements that govern flow in colloidal glasses, Science 318 (5858) (2007) 1895–1899, https://doi.org/10.1126/science.1149308 ⟨http://science.sciencemag.org/content/318/5858/1895.full.pdf⟩ http://science.sciencemag.org/content/318/5858/1895.

[93] G. Molnar, P. Ganster, A. Tanguy, Effect of composition and pressure on the shear strength of sodium silicate glasses: an atomic scale simulation study, Phys. Rev. E 95 (4) (2017) 043001, https://doi.org/10.1103/PhysRevE.95.043001

[94] A. Tanguy, Elasto-plastic behavior of amorphous materials: a brief review, Comptes Rendus. Phys. 22 (S3) (2021) 117–133, https://doi.org/10.5802/crphys.49

[95] M.J. Demkowicz, A.S. Argon, Autocatalytic avalanches of unit inelastic shearing events are the mechanism of plastic deformation in amorphous silicon, Phys. Rev. B 72 (24) (2005) 245206, https://doi.org/10.1103/PhysRevB.72.245206

[96] D. Srolovitz, V. Vitek, T. Egami, An atomistic study of deformation of amorphous metals, Acta Metall. 31 (2) (1983) 335–352 ⟨https://www.sciencedirect.com/science/article/pii/0001616083901104⟩.

[97] Y.C. Cheng, E. Ma, Atomic-level structure and structure-property relationship in metallic glasses, Prog. Mater. Sci. 56 (4) (2011) 379–473, https://doi.org/10.1016/j.pmatsci.2010.12.002

[98] D. Pan, A. Inoue, T. Sakurai, M.W. Chen, Experimental characterization of shear transformation zones for plastic flow of bulk metallic glasses, Proc. Natl. Acad. Sci. 105 (39) (2008) 14769–14772, https://doi.org/10.1073/pnas.0806051105

[99] D. Şopu, A. Stukowski, M. Stoica, S. Scudino, Atomic-level processes of shear band nucleation in metallic glasses, Phys. Rev. Lett. 119 (19) (2017) 195503, https://doi.org/10.1103/PhysRevLett.119.195503

[100] D. Şopu, S. Scudino, X.L. Bian, C. Gammer, J. Eckert, Atomic-scale origin of shear band multiplication in heterogeneous metallic glasses, Scr. Mater. 178 (2020) 57–61 ⟨http://www.sciencedirect.com/science/article/pii/S1359646219306499⟩.

[101] H. Luo, H. Sheng, H. Zhang, F. Wang, J. Fan, J. Du, J. Ping Liu, I. Szlufarska, Plasticity without dislocations in a polycrystalline intermetallic, Nat. Commun. 10 (2019) 3587.

[102] A. Misra, H. Jiang, Measured kinematic fields in the biaxial shear of granular materials (theoretical and Experimental Methods for Particulate Materials), Comput. Geotech. 20 (3–4) (1997) 267–285, https://doi.org/10.1016/S0266-352X(97)00006-2 (theoretical and Experimental Methods for Particulate Materials), ⟨http://www.sciencedirect.com/science/article/pii/S0266352×97000062⟩.

[103] P.-C. Kiatkirakajorn, L. Goehring, Formation of shear bands in drying colloidal dispersions, Phys. Rev. Lett. 115 (8) (2015) 088302, https://doi.org/10.1103/PhysRevLett.115.088302

[104] K.P. Krishnaraj, P.R. Nott, A dilation-driven vortex flow in sheared granular materials explains a rheometric anomaly, Nat. Commun. 7 (2016) 10630, https://doi.org/10.1038/ncomms10630

[105] I. Kriuchevskyi, J.P. Wittmer, O. Benzerara, H. Meyer, J. Baschnagel, Numerical determination of shear stress relaxation modulus of polymer glasses, Eur. Phys. J. E 40 (4) (2017), https://doi.org/10.1140/epje/i2017-11535-3

[106] M. Oda, H. Kazama, Microstructure of shear bands and its relation to the mechanisms of dilatancy and failure of dense granular soils, Géotechnique 48 (4) (1998) 465–481, https://doi.org/10.1680/geot.1998.48.4.465

[107] J.R. Williams, N. Rege, Coherent vortex structures in deforming granular materials, Mech. Cohes. -Frict. Mater. 2 (3) (1997) 223–236, https://doi.org/10.1002/(SICI)1099-1484(199707)2:3<223::AID-CFM30>3.0.CO;2-F

[108] Y. Forterre, O. Pouliquen, Longitudinal vortices in granular flows, Phys. Rev. Lett. 86 (26) (2001) 5886–5889, https://doi.org/10.1103/PhysRevLett.86.5886

[109] A.L. Rechenmacher, S. Abedi, O. Chupin, A.D. Orlando, Characterization of mesoscale instabilities in localized granular shear using digital image correlation, Acta Geotech. 6 (4) (2011) 205–217, https://doi.org/10.1007/s11440-011-0147-2

[110] H. Rösner, M. Peterlechner, C. Kübel, V. Schmidt, G. Wilde, Density changes in shear bands of a metallic glass determined by correlative analytical transmission electron microscopy, Ultramicroscopy 142 (2014) 1–9 ⟨https://www.sciencedirect.com/science/article/pii/S0304399114000515⟩.

[111] V. Hieronymus-Schmidt, H. Rösner, G. Wilde, A. Zaccone, Shear banding in metallic glasses described by alignments of eshelby quadrupoles, Phys. Rev. B 95 (2017) 134111, https://doi.org/10.1103/PhysRevB.95.134111

[112] S. Kang, D. Wang, A. Caron, C. Minnert, K. Durst, C. Kübel, X. Mu, Direct observation of quadrupolar strain fields forming a shear band in metallic glasses (n/a(n/a)), Adv. Mater. (2023) 2212086, https://doi.org/10.1002/adma.202212086

[113] A. Stukowski, Visualization and analysis of atomistic simulation data with ovito-the open visualization tool, Modell. Simul. Mater. Sci. Eng. 18 (1) (2010) 015012.

[114] D. Şopu, X. Yuan, F. Moitzi, F. Spieckermann, X. Bian, J. Eckert, From elastic excitations to macroscopic plasticity in metallic glasses, Appl. Mater. Today 22 (2021) 100958⟨https://www.sciencedirect.com/science/article/pii/S2352940721000238⟩.

[115] S. Wang, M. Kramer, M. Xu, S. Wu, S. Hao, D. Sordelet, K. Ho, C. Wang, Experimental and ab initio molecular dynamics simulation studies of liquid Al/sub 60/Cu/sub 40/ alloy, Phys. Rev. B: Condens. Matter 79 (14) (2009) 1442059 pp..

[116] T. Egami, T. Iwashita, W. Dmowski, Mechanical properties of metallic glasses (2013).

[117] S. Scudino, D. Şopu, Strain distribution across an individual shear band in real and simulated metallic glasses, Nano Lett. 18 (2) (2018) 1221–1227, https://doi.org/10.1021/acs.nanolett.7b04816

[118] A.S. Argon, Mechanisms of inelastic deformation in metallic glasses, J. Phys. Chem. Solids 43 (10) (1982) 945–961 ⟨https://www.sciencedirect.com/science/article/pii/0022369782901111⟩.

[119] S. Scudino, J.J. Bian, H. ShakurShahabi, D. Şopu, J. Sort, J. Eckert, G. Liu, Ductile bulk metallic glass by controlling structural heterogeneities, Sci. Rep. 8 (2018) 9174, https://doi.org/10.1038/s41598-018-27285-5

[120] M. Hassani, A.E. Lagogianni, F. Varnik, Probing the degree of heterogeneity within a shear band of a model glass, Phys. Rev. Lett. 123 (19) (2019) 195502, https://doi.org/10.1103/PhysRevLett.123.195502

[121] K. Kosiba, S. Scudino, J. Bednarcik, J. Bian, G. Liu, U. Kühn, S. Pauly, Guiding shear bands in bulk metallic glasses using stress fields: a perspective from the activation of flow units, Phys. Rev. B 102 (13) (2020) 134113, https://doi.org/10.1103/PhysRevB.102.134113

[122] D. Şopu, F. Moitzi, N. Mousseau, J. Eckert, An atomic-level perspective of shear band formation and interaction in monolithic metallic glasses, Appl. Mater. Today 21 (2020) 100828⟨http://www.sciencedirect.com/science/article/pii/S2352940720302766⟩.

[123] H. Sheng, D. Şopu, S. Fellner, J. Eckert, C. Gammer, Mapping shear bands in metallic glasses: from atomic structure to bulk dynamics, Phys. Rev. Lett. 128 (24) (2022) 245501, https://doi.org/10.1103/PhysRevLett.128.245501

[124] J. Luo, L. Huang, Y. Shi, B. Deng, The dynamics of shear band propagation in metallic glasses, Acta Mater. 248 (2023) 118787⟨https://www.sciencedirect.com/science/article/pii/S1359645423001180⟩.

[125] X. Mu, M.R. Chellali, E. Boltynjuk, D. Gunderov, R.Z. Valiev, H. Hahn, C. Kübel, Y. Ivanisenko, L. Velasco, Unveiling the local atomic arrangements in the shear band regions of metallic glass, Adv. Mater. 33 (12) (2021) 2007267, https://doi.org/10.1002/adma.202007267

[126] L.-Q. Shen, J.-H. Yu, X.-C. Tang, B.-A. Sun, Y.-H. Liu, H.-Y. Bai, W.-H. Wang, Observation of cavitation governing fracture in glasses, Sci. Adv. 7 (14) (2021) eabf7293, https://doi.org/10.1126/sciadv.abf7293

[127] F. Moitzi, D. Şopu, D. Holec, D. Perera, N. Mousseau, J. Eckert, Chemical bonding effects on the brittle-to-ductile transition in metallic glasses, Acta Mater. 188 (2020) 273–281 ⟨http://www.sciencedirect.com/science/article/pii/S135964542030094X⟩.

[128] X. Yuan, D. Şopu, F. Moitzi, K.K. Song, J. Eckert, Intrinsic and extrinsic effects on the brittle-to-ductile transition in metallic glasses, J. Appl. Phys. 128 (12) (2020) 125102, https://doi.org/10.1063/5.0020201

[129] H. Gleiter, Nanoglasses: a new kind of noncrystalline material and the way to an age of new technologies? Small 12 (16) (2013) 2225–2233, https://doi.org/10.1002/smll.201500899

[130] X.L. Bian, D. Zhao, J.T. Kim, D. Şopu, G. Wang, R. Pippan, J. Eckert, Controlling the distribution of structural heterogeneities in severely deformed metallic glass, Mater. Sci. Eng.: A 752 (2019) 36–42 ⟨https://www.sciencedirect.com/science/article/pii/S0921509319302606⟩.

[131] Z.F. Zhang, J. Eckert, L. Schultz, Difference in compressive and tensile fracture mechanisms of Zr59Cu20Al10Ni8Ti3 bulk metallic glass, Acta Mater. 51 (4) (2003) 1167–1179, https://doi.org/10.1016/s1359-6454(02)00521-9

[132] X.D. Wang, J. Bednarcik, K. Saksl, H. Franz, Q.P. Cao, J.Z. Jiang, Tensile behavior of bulk metallic glasses by in situ x-ray diffraction, Appl. Phys. Lett. 91 (8) (2007) 81913, https://doi.org/10.1063/1.2773945

[133] C. Schuh, T. Hufnagel, U. Ramamurty, Mechanical behavior of amorphous alloys, Acta Mater. 55 (12) (2007) 4067–4109, https://doi.org/10.1016/j.actamat.2007.01.052

[134] R. Raghavan, P. Murali, U. Ramamurty, On factors influencing the ductile-to-brittle transition in a bulk metallic glass, Acta Mater. 57 (11) (2009) 3332–3340, https://doi.org/10.1016/j.actamat.2009.03.047

[135] P. Murali, U. Ramamurty, V.B. Shenoy, Factors influencing deformation stability of binary glasses, J. Chem. Phys. 128 (10) (2008) 104508, https://doi.org/10.1063/1.2839300

[136] N. Mousseau, L.K. Béland, P. Brommer, J.-F. Joly, F. El-Mellouhi, E. Machado-Charry, M. Marinica, P. Pochet, The activation-relaxation technique: art nouveau and kinetic art, J. At., Mol. Opt. Phys. 2012 (2012) 1–14, https://doi.org/10.1155/2012/925278

[137] J. Pan, Y.P. Ivanov, W.H. Zhou, Y. Li, A.L. Greer, Strain-hardening and suppression of shear-banding in rejuvenated bulk metallic glass, Nature 578 (7796) (2020) 559–562, https://doi.org/10.1038/s41586-020-2016-3

[138] C. Liu, R. Maaß, Elastic fluctuations and structural heterogeneities in metallic glasses, Adv. Funct. Mater. 28 (30) (2018) 1800388, https://doi.org/10.1002/adfm.201800388

[139] P. Ross, S. Küchemann, P.M. Derlet, H. Yu, W. Arnold, P. Liaw, K. Samwer, R. Maaß, Linking macroscopic rejuvenation to nano-elastic fluctuations in a metallic glass, Acta Mater. 138 (2017) 111–118 ⟨http://www.sciencedirect.com/science/article/pii/S1359645417306055⟩.

[140] M.Q. Jiang, G. Wilde, J.H. Chen, C.B. Qu, S.Y. Fu, F. Jiang, L.H. Dai, Cryogenic-temperature-induced transition from shear to dilatational failure in metallic glasses, Acta Mater. 77 (2014) 248–257 ⟨https://www.sciencedirect.com/science/article/pii/S135964541400408X⟩.

[141] W.H. Wang, Dynamic relaxations and relaxation-property relationships in metallic glasses, Prog. Mater. Sci. 106 (2019) 100561⟨http://www.sciencedirect.com/science/article/pii/S0079642519300295⟩.